Performance Evaluation and Optimization of a Photovoltaic/Thermal (PV/T) System according to Climatic Conditions

Ehsanolah Assareh [1,*], Masoud Jafarian [2], Mojtaba Nedaei [3,*], Mohammad Firoozzadeh [4,5] and Moonyong Lee [1,*]

1   School of Chemical Engineering, Yeungnam University, Gyeongsan 38541, Korea
2   Department of Mechanical Engineering, Dezful Branch, Islamic Azad University, Dezful 313, Iran
3   Department of Management and Engineering, University of Padua, 36100 Vicenza, Italy
4   Department of Mechanical Engineering, Jundi-Shapur University of Technology, Dezful 334-64615, Iran
5   Jundi-Shapur Research Institute, Jundi-Shapur University of Technology, Dezful 334-64615, Iran
*   Correspondence: ehsanolah.assareh@yu.ac.kr (E.A.); mojtaba.nedaei@phd.unipd.it (M.N.); mynlee@yu.ac.kr (M.L.)

Abstract: Population and economic growth, industrial activities, development of technology, and depletion of fossil fuels have all led to increasing energy demand. As a result, there is an increasing ambition towards implementation of sustainable energy sources. In this study, first, a review of the literature is conducted to learn about various methods and objectives for optimization of photovoltaic and thermal (PV/T) systems. Then, a case study is considered, and the seasonal and hourly solar radiation are studied. Further, two methods of multiobjective evolutionary algorithm based on decomposition (MOEA/D) and multiobjective particle swarm optimization (MOPSO) are compared. On this basis, the energy and exergy efficiencies are analyzed for a proposed PV/T system. The outcomes are validated by taking into account the previous studies, and a sufficient agreement is found indicating the validity and accuracy of the results. It is also found that the efficiency rates for both energy and exergy soar with a rise in the ambient temperature. Additionally, a growth in the warm water flow rate from 0.4 to 1 kg/s increases the exergy efficiency by 0.6%. It is concluded that the MOEA/D method outperforms the MOPSO in terms of the optimization of the proposed PV/T system.

Keywords: optimization; MOEA/D; MOPSO; PV/T; energy; exergy; efficiency

1. Introduction

Today, political and economic crises, limited fossil fuel resources, high energy price, population growth, and consumption growth have all stimulated planners to think of more efficient alternatives for traditional power sources. Sustainable energy is clean and cost-effective. An efficient renewable energy source is solar power. Two forms of solar energy systems can be utilized, i.e., thermal systems and PV systems. The former converts sunlight into heat while the latter converts sunlight into electricity power. Typically, such systems are utilized in a separate manner. However, in a photovoltaic/thermal (PV/T) setup, both electricity and heat can practically be harnessed. Therefore, these systems have higher energy and exergy efficiencies compared with PV modules and solar thermal systems, and this has been confirmed by many scholars.

The integration possibility of solar energy has been grounds for many studies to undertake optimization of exergy and energy. Exergy analysis, according to the second rule of thermodynamics, is a fundamental process in order to study the power systems. In addition, it explains thermodynamically ineffective and unsuitable processes. Exergy has recently become a cornerstone to achieve a better insight into the processes, inefficient resource quantities, and quality detection of energy consumption [1,2].

Large-scale building-integrated photovoltaic/thermal (BIPV/T) systems incorporating façade as well as roof can be developed in EnergyPlus and TRNSYS. Vuong et al. [3] concluded that what make the outcome between EnergyPlus and TRNSYS different are model calculations regarding weather data, sky temperature, and electricity. In order to meet annual demand and decrease energy consumption in buildings, Xu et al. [4] introduced a novel BIPV/T system. During the summer, the system offers passive cooling with efficiency of 7.6%, whilst in winter it offers heating with efficiency of 12.5%. In order to enhance the heat transfer between photovoltaic modules and flowing air, a novel BIPV/T system was proposed by Yang and Athienitis [5]. It was shown that the thermal efficiency is, respectively, 5% and 7.6% more by considering two inlets, rather than one, and utilizing semitransparent, compared to opaque, PV.

There are two ways to determine the best performance point of each PV/T system; performing a lot of experiments and using intelligent computer methods. Nowadays, computer methods can direct us to discovering the best solution for each complex system rapidly and more accurately [6]. Shahsavar et al. [7] focused on several designated variables, e.g., channel depth, length, width, and the outlet air temperature of the channel in an air-based PV/T system. They used the non-dominated sorting genetic algorithm (NSGA) to optimize the system and reported the best cases. In addition, the optimal case was weighed and examined according to the experimental data, and a sufficient compatibility was shown. In another study, Cao et al. [8] studied a PV system cooled with a nanofluid. They investigated the impacts of three major variations of the nanofluid properties, solar irradiation, and the nanofluid flow rate. The adaptive neuro-fuzzy inference system (ANFIS) was utilized in order to optimize the system, and the optimum electrical efficiency of the considered system was estimated.

On the basis of the literature review analysis, a few studies in the area of optimization of PV/T systems were carried out. A novel optimization methodology for specific use in a microchannel was presented by Karathanassis et al. [9] in 2013. The model can be used for a linear parabolic trough concentrating photovoltaic system, cooled by plate-fins. The thermal resistance of the utilized plate-fins was also considered in their assessments. Khaki et al. [10] adopted the genetic algorithm (GA) to improve energy together with exergy in BIPV/T systems. As a result, higher efficiencies were observed. Vera et al. [11] proposed a mathematical model and predicted the efficiency of a BIPV/T system both mathematically and experimentally. They employed the GA to determine the best decision parameters having influence on the system's mechanism and general operation. The following parameters were investigated: air gap, aspect ratio, collector's length, number of collectors, fluid mass-flow rate, and storage tank capacity. Singh et al. [12] focused on using the GA incorporated with the optimization goals to enhance the overall efficiency of a PV/T system in New Delhi in India by considering the climatic factors. Sohani et al. [13] performed multiobjective optimization of a BIPV/T system incorporating the phase change material (PCM), under the climate of Tehran, capital of Iran. The optimization was performed in terms of energy, environment, and economics. As a result, the optimal thickness of the PCM for the test conditions was found to be 77.2 mm. Moreover, 17.7% lower CO_2 was annually emitted in comparison to the base case, and the energy payback period of the system was discovered to be 3.3 years. Sarhaddi et al. [14] analyzed the operation of a PV/T setup. They presented a new technique to study the design parameters of a typical air-based PV/T setup. In addition, the general energy analysis of an air-based PV/T setup was performed by considering electrical, thermal, and environmental parameters. Their results indicated that the overall energy, electrical, and thermal efficiencies of the investigated system were approximately 45%, 10%, and 17.18%, respectively. In the most recent study, in 2022, Sattar et al. [15] performed an analytical model for a photovoltaic module integrated with the air flow as a coolant. The main considered parameters were cell temperature, irradiation, and mass flow rate, as well as the duct geometrical specifications. Moreover, the primary optimizing goal was to maximize the output electrical power. To achieve this objective, a multiobjective multivariable optimization was applied to the system. As result,

a multipass duct with 31 passes and with the mass flow rate of 0.14 kg/s was introduced as the optimum case, resulting in the maximum electrical output power of 186.7 W.

The purpose of the current research is to find the most appropriate method to optimize a PV/T system according to multiobjective optimization. Another goal is to study the performance evaluation of a proposed PV/T system by considering the climate of Ilam, Iran, as a case study. For these purposes, a new approach according to a multiobjective evolutionary algorithm based on decomposition (MOEA/D) along with multiobjective particle swarm optimization (MOPSO) is developed. The proposed method maximizes the effectiveness of a PV/T system from a novel perspective.

2. Methodology

2.1. Multiobjective Particle Swarm Optimization (MOPSO)

There are a wide variety of methods for optimization purposes. Among these methods, MOPSO is one of the most efficient techniques due to its simple implementation and adequate convergence speed. Table 1 shows the framework of the MOPSO algorithm:

Table 1. Framework of the MOPSO.

Particle initialization	→	P
Create archive	→	A
While	→	Stopping criteria is not satisfied
Evaluate(P)	→	P
Update(A)	→	A
Select pbest(P)	→	P
Select gbest(P)	→	P
Update(P)	→	P
End	→	While

Where pbest is the personal best position determined by a designated particle, and gbest is the global best position considered by the whole swarm of particles [16].

2.2. Multiobjective Evolutionary Algorithm Based on Decomposition (MOEA/D)

Decomposition has widely been utilized in mathematics for the purpose of investigating the multiobjective optimization problems (MOPs). As a matter of fact, most multiobjective evolutionary algorithms (MEAs) treat an MOP in an overall manner and primarily depend on domination for determining the solution quality during their search. Such methods are not appropriate for producing an even distribution of solution along the Pareto front. MOEA/D adopts a decomposition approach to distribute the MOP into a series of scalar optimization issues. Every individual solution in the population of MOEA/D is linked with a subprocedure or subproblem. A neighborhood association among all the subprocedures is established according to the lengths of their weight vectors. In MOEA/D, enhancement of a subprocedure utilizes the existing data of its neighboring subprocedures because two neighboring subprocedures should have the best solutions that are close to one another. Complete formulations of the algorithm are fully described in [17].

2.3. Thermal Analysis

For the purpose of thermal analysis, the following assumptions were considered:
- The flow is steady and constant.
- All of the components are considered adiabatic.

The energy equilibrium equations of PV/T components with thermal parameters and the thermal efficiency are written as

$$T_{cell} = \frac{(\tau\alpha)_{eff}I_s + U_{top}T_{amb} + U_T T_p}{U_{top} + U_T} \tag{1}$$

where T_{cell} is the solar cell temperature, τ is transmissivity, α is absorptivity, I_s is incident solar intensity, U_{top} represents the net heat transfer coefficient from the solar cell to the ambient atmosphere by considering the glass, T_{amb} represents the ambient air temperature, U_T represents the heat transfer coefficient from solar cell to ambient through glass cover, and T_p represents the plate temperature [18].

For the purpose of estimating the thermal efficiency of the PV/T, η_{th}, the heat, Q, is estimated according to the following equation:

$$Q = \dot{m}C_p(T_0 - T_i) \tag{2}$$

where $\dot{m}$ is the rate for the mass flow, C_p is indicative of the specific heat, and T_0 and T_i, are the temperatures of the fluid situated at the outlet and inlet of the heat absorbing unit.

The thermal efficiency of the PV/T system, η_{th}, can be defined according to Equations (3) and (4):

$$\eta_{th} = \frac{Q}{A.S_r} \tag{3}$$

$$\eta_{th} = \eta_0 - H_l \left(\frac{T_i - T_a}{S_r} \right) \tag{4}$$

where Q is the collected heat, A is the collector area, S_r is the solar radiation, η_0 is the thermal efficiency in the occasion that $|T_i - T_a| = 0$, and H_l is the heat loss factor [19].

2.4. Electrical Efficiency

The electrical efficiency, η_e, can be calculated according to Equations (5) and (6):

$$P_{max} = V_{oc} \times I_{sc} \times FF \tag{5}$$

$$\eta_e = \frac{P_{max}}{A.S_r} \tag{6}$$

where P_{max} is the highest level of electrical power, V_{oc} is the open-circuit voltage, I_{sc} is the short-circuit current, and FF is the fill factor [19].

2.5. Overall Energy Efficiency

The overall energy efficiency, η_o, is defined as the sum of thermal and electrical efficiecies [19]:

$$\eta_o = \eta_{th} + \eta_e \tag{7}$$

2.6. Exergy Analysis

Exergy, which is indicative of the second rule of thermodynamics, is expressed as the highest effective activity that is hypothetically accessible from a thermodynamic system. Hence, the exergy efficiency of a PV/T collector is explained according to the allocation of this highest theoretically accessible output that can be considered as an actual intended output. Further to the electrical and thermal efficiencies, the exergy efficiency is also calculated, as this definitely leads to a more realistic indication of the system's operation. The exergy efficiency of a PV/T system is defined as follows:

$$\sum \dot{Ex}_{out} = \sum \dot{Ex}_{thermal} + \sum \dot{Ex}_{electrical} \tag{8}$$

where $\dot{Ex}_{out}$, $\dot{Ex}_{thermal}$, and $\dot{Ex}_{electrical}$ are the total output exergy rate, thermal, and electrical exergy, in the order given.

$$\sum \dot{Ex}_{in} = A \times SR \times [1 - \frac{4}{3} \times (\frac{T_a}{T_s}) + \frac{1}{3} \times (\frac{T_a}{T_s})^4] \tag{9}$$

where $\dot{Ex}_{in}$ is the total input exergy rate, and T_a and T_s are ambient and surface temperatures in °C.

$$\sum \dot{Ex}_{thermal} = \dot{Q}_u[1 - \frac{T_a + 273}{T_{out} + 273}] \tag{10}$$

$$\sum \dot{Ex}_{electrical} = I_{mp} \times V_{mp} \tag{11}$$

$$\eta_{ex} = \frac{\sum \dot{Ex}_{out}}{\sum \dot{Ex}_{in}} \tag{12}$$

where $\dot{Q}_u$ is the rate of practical and effective heat absorbed by the module, I_{mp} is the maximum current of the panel, V_{mp} is the maximum voltage of the panel, and η_{ex} is the PV/T collector exergy efficiency [20].

2.7. Schematic of the Proposed System

The illustration of the proposed PV/T system is explained according to Figure 1. In this system, the thermal output of the PV/T panel is linked with the thermal system, which produces hot water. The system's fluid is flowed and moved round by a pump.
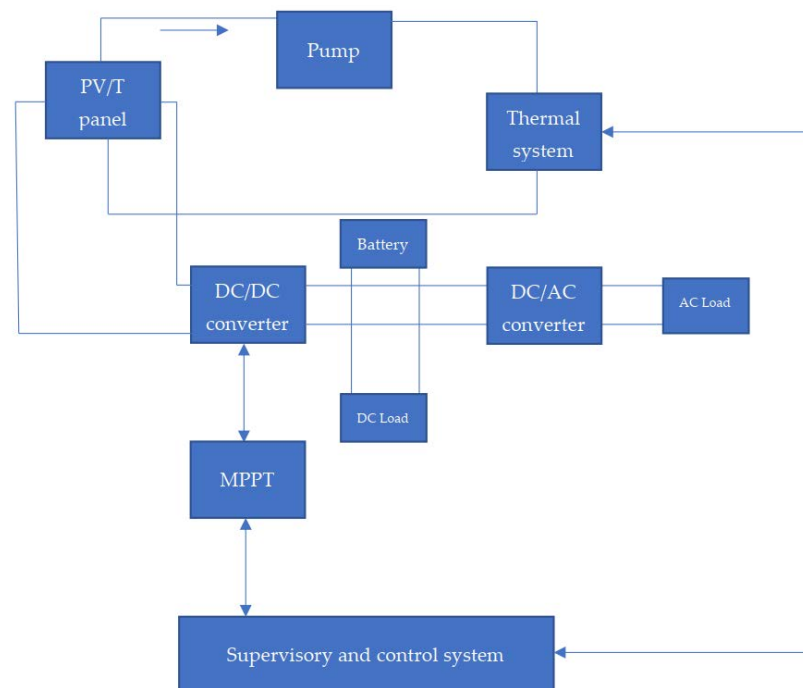

Figure 1. The demonstration of the proposed PV/T system.

2.8. Analysis of the Sunlight Data

The sunlight per square meter, which is the most important parameter of a photovoltaic module, should be estimated to specify the power as well as heat generated by the solar panel. Figure 2 shows the sunlight data estimated according to [21] for all hours and seasons.
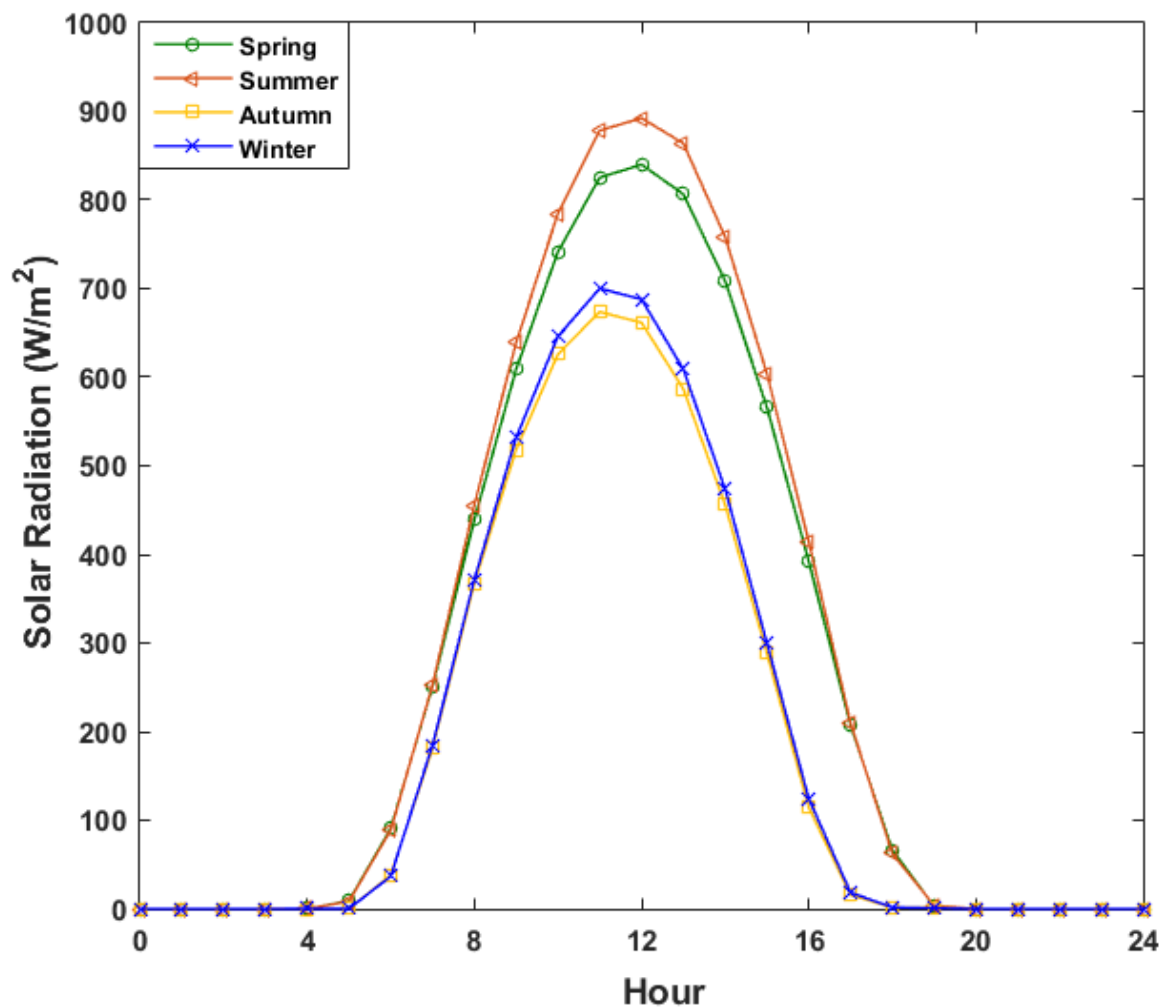
Figure 2. Solar irradiation data for Ilam (Iran).

3. Results and Discussion

This study discusses the thermodynamic analysis of a PV/T system according to the first and second rules of thermodynamics. The proposed system's outcomes are evaluated according to different design conditions.

To validate the proposed mathematical model, the photovoltaic module temperature and output air temperature were examined according to the data of Ref. [10], as shown in Figure 3. Clearly, it is inferred that the outcomes of this study and those of [10] are in good agreement. Hence, the validity of the presented approach is shown. The model can therefore be used to simulate, optimize, and analyze the electrical and thermal aspects of the proposed PV/T system. Table 2 shows the calculated errors. The lower the error rate, the more precise the results are.
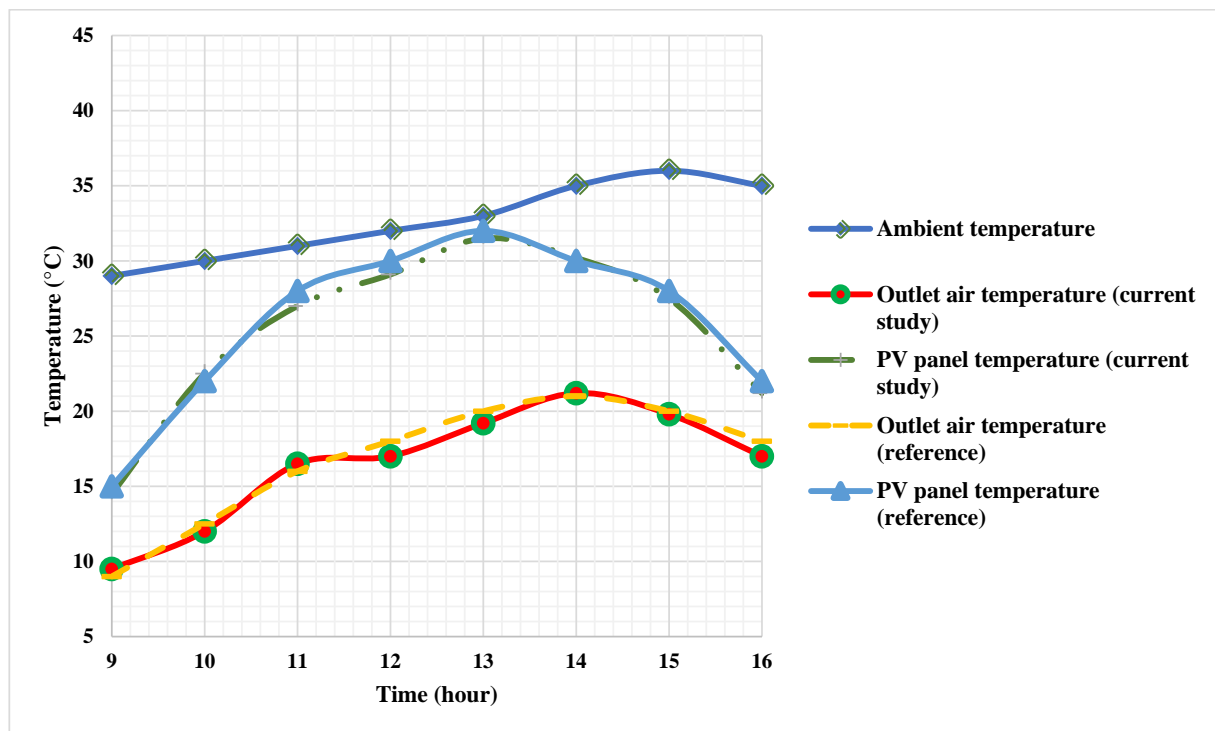
Figure 3. Evaluation of the validity of the results by comparing the current results and the results of the studied reference.

Table 2. Calculated errors for the studied parameters.

Hour	Error Regarding the Photovoltaic Panel Temperature (%)	Error in Case of Outlet Air Temperature (%)
9	0.005	0.005
10	0.005	0.005
11	0.01	0.005
12	0.009	0.01
13	0.005	0.008
14	0.002	0.002
15	0.005	0.002
16	0.008	0.01

Figure 4 depicts the heat generation of the photovoltaic system for different hours and different seasons. As can be seen, the solar panels generated more heat during sunny hours.

Figure 5 illustrates the proposed system's power generation. According to Figure 5, power generation increased as sunlight enhanced during the day, when the PV/T system was in operation. Additionally, power and heat generation decreased as sunlight declined in cold seasons. The generation of no power at night was another result. Given that a large portion of power is consumed by buildings and the peak power consumption time is 16:00–22:00, a support or storage system should be employed at nights.
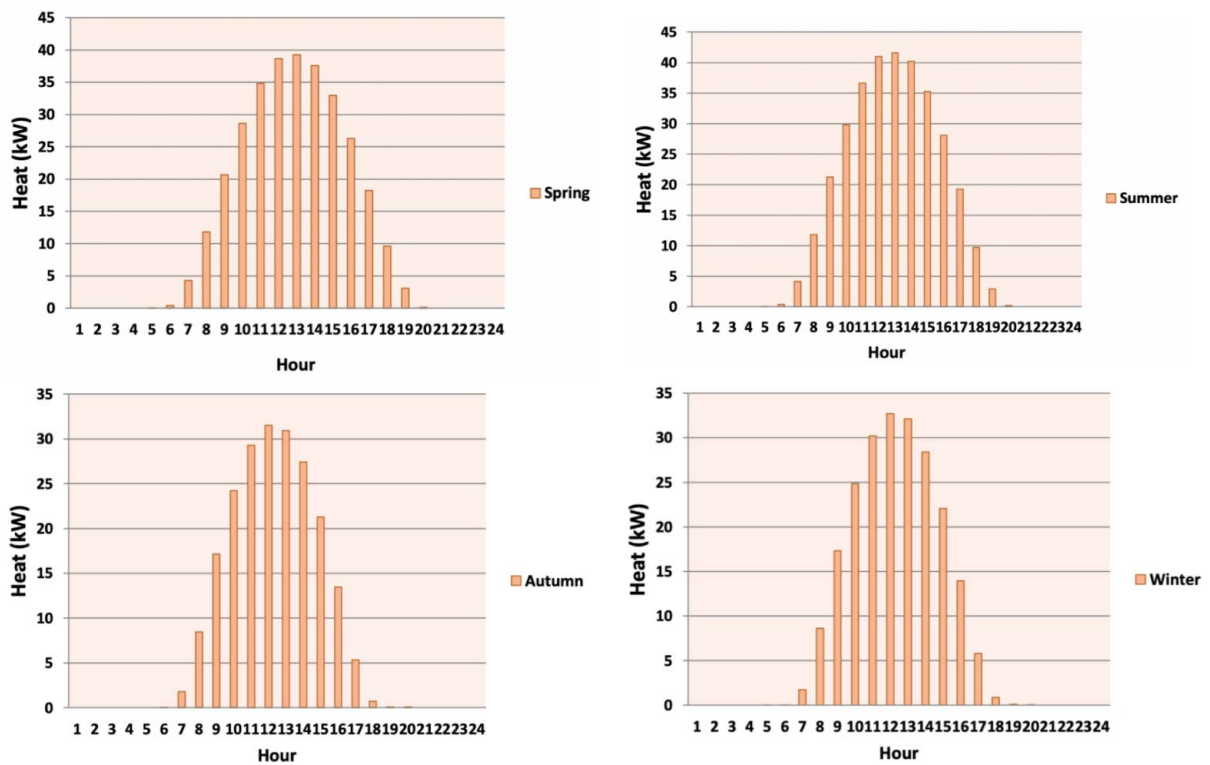
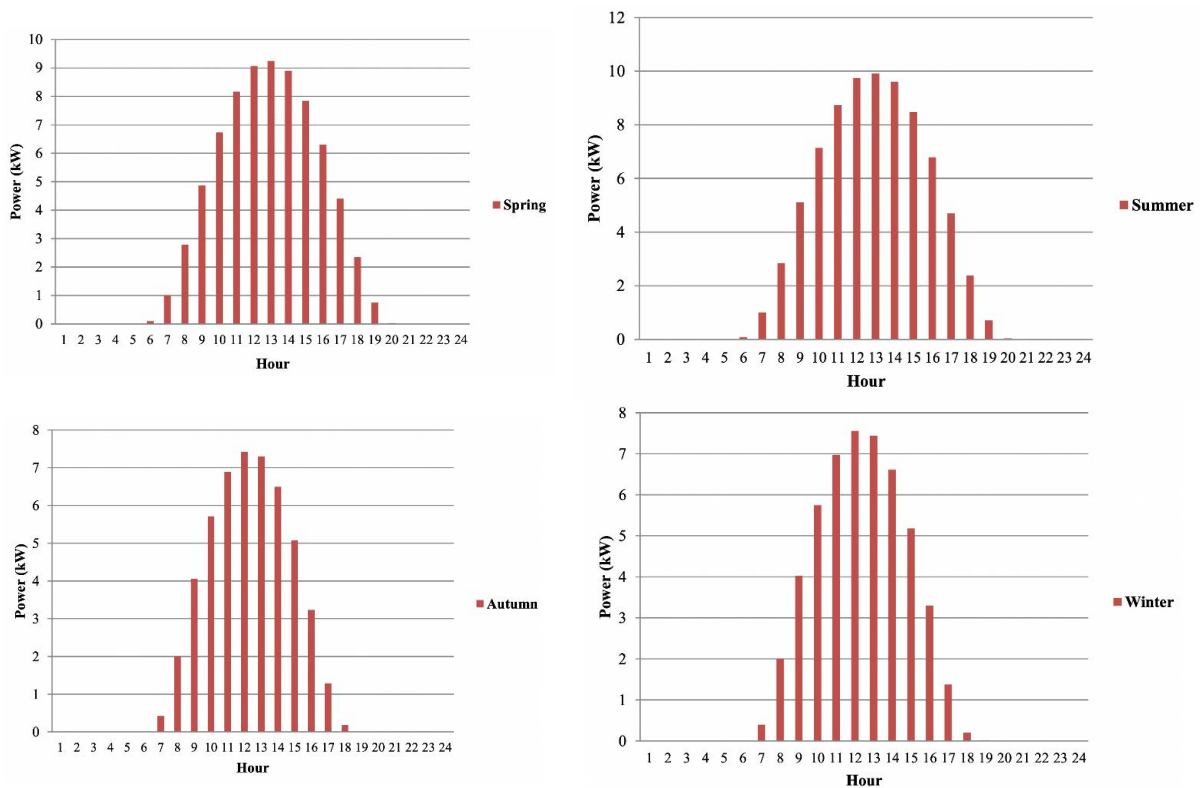**Figure 4.** PV/T heat generation distribution based on time.

Figure 5. PV/T electricity power generation distribution based on time.

The electrical efficiency of the PV/T system at different hours and in different seasons is depicted in Figure 6. A solar panel's efficiency is dependent on environmental conditions, including sunlight, and the panel type. As expected, the electrical efficiency is zero when

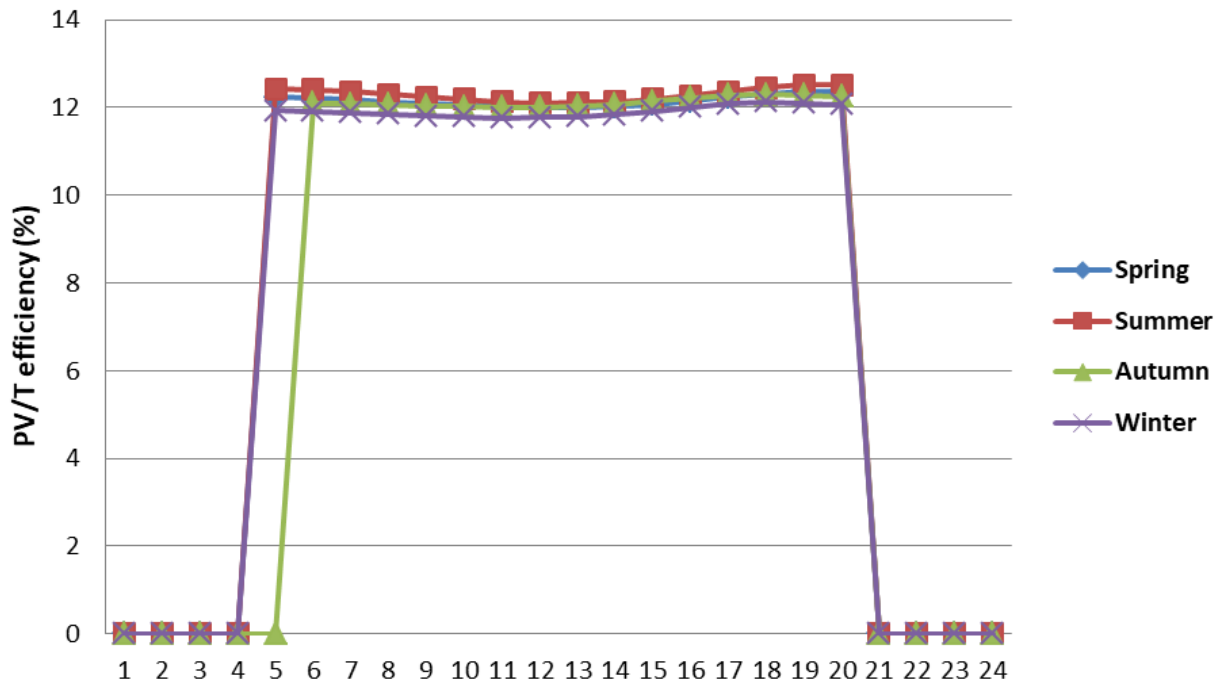there is no sunlight, and it slightly changes in the remaining hours due to the sunlight and its angle.

Figure 6. The electrical efficiency of the proposed PV/T system.

Both energy and exergy efficiencies increased as the ambient temperature increased, as depicted in Figure 7. The energy efficiency rose by approximately 2% as the ambient temperature increased from −10 °C to 30 °C. The exergy efficiency was increased by more than 2% by the same change in the ambient temperature.
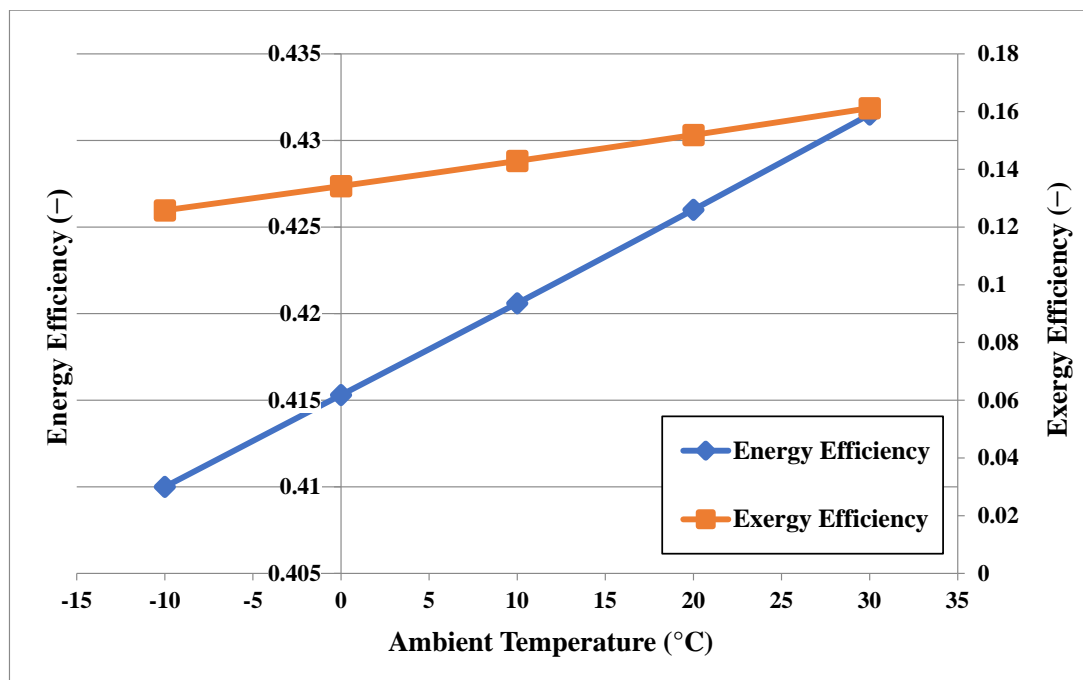

Figure 7. Energy and exergy efficiencies versus ambient temperature.

Additionally, the exergy efficiency was enhanced as the warm water flow rate of the panels was increased. A rise in the warm water flow rate from 0.4 to 1 kg/s increased the

exergy efficiency by 0.6%. The energy efficiency was reduced by more than 20% by the rise of the warm water flow rate. This is depicted in Figure 8.
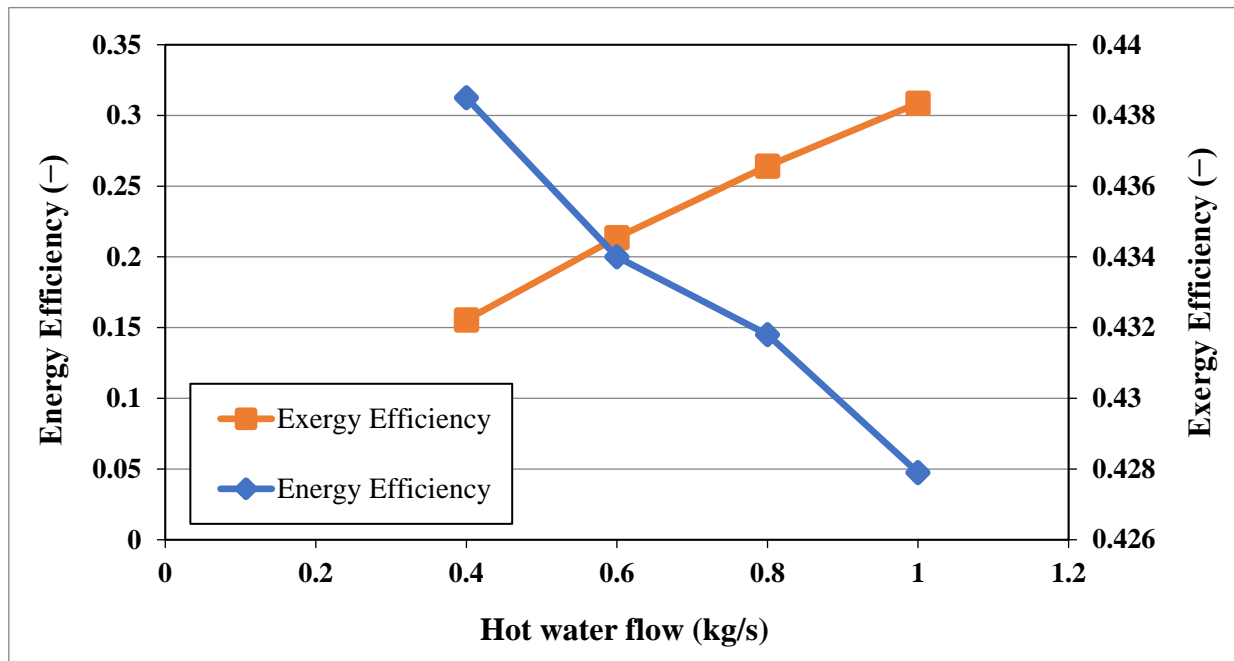

Figure 8. Energy and exergy efficiencies versus the flow rate of the hot water.

Table 3 provides the decision variables that influence the objective function along with acceptable values to maximize the exergy and energy efficiencies at the same time.

Table 3. Design parameters and their variation ranges for optimization.

Parameters	Symbol	Lower Limit	Upper Limit
Number of PV panels	N_{Panel} (−)	0	200
Warm water flow rate	m_d (kg/s)	0	3
Solar irradiation	I (W/m^2)	0	900
Ambient temperature	T (°C)	−20	40

As a result, the objective functions reached their highest values by changing the variables shown in Table 3. The optimal point was also identified. The diagram in Figure 9 was obtained by dual-objective optimization and its purpose is to achieve satisfactory levels of the design variables as well as the optimization goals, including energy and exergy efficiencies. It divides the solution space into two domains: an acceptable domain and an unacceptable domain. The ideal point of the curve is the one with the highest energy and exergy efficiencies. According to Figure 9, a spot on the diagram with the shortest length from the ideal point is the optimal region. The diagram illustrates the optimal points of the two objective functions. The optimization of the PV/T system is fulfilled by the MOPSO and MOEA/D methods in the same conditions. In general, the optimal point of the exergy efficiency was found to be approximately 1.23% higher in the MOEA/D method than in the MOPSO method. In addition, the optimal point of the energy efficiency was 1.9% larger in the MOEA/D approach than in the MOPSO approach. Thus, it is indicated that the MOEA/D method can be more suitable for the multiobjective optimization of the PV/T system.
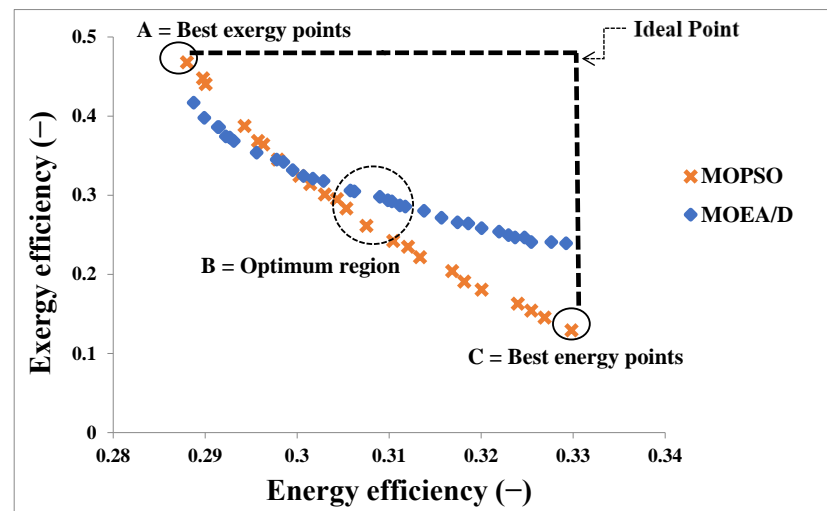
Figure 9. Comparing the optimal points between the MOPSO and MOEA/D approaches.

According to Figure 9, an increase in the energy efficiency decreases the exergy efficiency. Given the exergy efficiency's behavior, it can be found that the excessive use of panels directly elevates the exergy efficiency. A decision-making process was employed to choose the final solution from the optimal points. According to Table 4, the maximum energy efficiency of 33% and the minimum exergy efficiency of 13% are observed at point C. In addition, the minimum energy efficiency of 29% and maximum exergy efficiency of 46% are obtained at point A. The satisfactory exergy efficiency is achieved by considering an objective function at point C.

Table 4. The optimal exergy and energy efficiency values for points A, B, and C at suitable Pareto parameters for the given inputs.

Parameter	(With Consideration of Heat Recovery)		
	A	**B (The Optimal Point)**	**C**
η_{ex}	0.468	0.290	0.129
η_{energy}	0.288	0.314	0.330

Table 5 shows decision variables at points A, B, and C. Clearly, an increase in the energy efficiency enhances the warm water flow rate in each panel and the number of panels. Thus, the exergy efficiency can increase by reducing the warm water flow rate and the number of panels when the objective is only to increase the exergy efficiency; however, this would reduce the energy efficiency. Moreover, reducing the number of panels in the given range and the hot air flow rate increases energy efficiency while decreasing the exergy efficiency. This suggests that a rise in the number of panels and the solar energy-receiving area increases the energy efficiency fraction's denominator such that it can be neutralized by the fraction's nominator—that is, the effective energy generation.

Table 5. Optimal parameters at points A, B, and C in the optimal Pareto front.

Parameter	A	B (The Optimal Point)	C
Number of PV panels	41	60	65
Warm water flow rate (kg/s)	0.478	0.433	0.450
Solar irradiation (W/m^2)	254	328	800
Ambient temperature (°C)	313	313	313

4. Conclusions

Solar energy is an affordable and easily accessible source of energy. To utilize solar energy effectively, it is necessary to absorb the sunlight by solar collectors and convert it into heat. With this perspective, this study investigated the multiobjective optimization

of a photovoltaic/thermal (PV/T) system. In order to achieve this goal, the most appropriate method of optimizing the proposed PV/T system was determined. In addition, the efficiency of the system under climatic conditions was studied. A case study of Ilam in Iran was considered. Solar radiation data for all seasons were analyzed. Then, heat and electricity generation distributions of the PV/T system were determined and studied. Then, in order to assess the proposed approach, the current results were verified according to the previous studies, and a proper agreement was found. Further, the decision variables that influence the objective functions were determined and their variations for optimization were examined.

The following results are highlighted:

- Solar collectors generated more heat during the sunny hours when the amount of sunlight was high. In addition, power generation was higher during days, when the PV/T system was in operation, due to higher sunlight. On the other hand, the reduction of sunlight in cold seasons decreased the proposed system's power and heat generation.
- The electrical efficiency of the solar panels slightly changed as the sunlight and its angle changed.
- Results showed that an increase in the energy efficiency decreased the exergy efficiency. Given the exergy efficiency's patterns, it was found that the excessive use of panels directly elevated the exergy efficiency.
- The optimal point for the energy efficiency of the MOEA/D method was approximately 1.23% higher than that of the MOPSO method. In addition, the exergy efficiency of the MOEA/D method was 1.9% higher than that of the MOPSO method.
- It was found that the MOEA/D method is more suitable for the multiobjective optimization of the PV/T system.

Author Contributions: E.A.: conceptualization, methodology, writing, software. M.J.: conceptualization and investigation. M.N.: writing, reviewing, editing, and revising. M.F.: writing, reviewing, editing, and revising. M.L.: writing, reviewing, editing, and revising. All authors have read and agreed to the published version of the manuscript.

Institutional Review Board Statement: Not applicable.

Informed Consent Statement: Not applicable.

Data Availability Statement: Not applicable.

Conflicts of Interest: The authors declare no conflict of interest.

Nomenclature

Mathematical notations:
Greek symbols:

Mathematical notation	Definition	Unit
α	Absorptivity	$Ws^{0.5}/m/k$
τ	Transmissivity	$W/m.k$

Greek symbols with subscripts:

Mathematical notation	Definition	Unit
η_{th}	Thermal efficiency	%
η_o	Overall energy efficiency	%
η_0	Thermal efficiency (note: this efficiency is considered in the occasion that $|T_i - T_a| = 0$)	%
η_e	Electrical efficiency	%
η_{ex}	PV/T collector exergy efficiency	%

Latin symbols:

Mathematical notation	Definition	Unit
A	Collector area	m^2
Q	Collected heat	J
S_r	Solar radiation	W/m^2

Latin symbols with subscripts:

Mathematical notation	Definition	Unit
H_l	Heat loss coefficient	Unitless
I_{mp}	Maximum current of the panel	A
I_{sc}	Short-circuit current	A
I_s	Incident solar intensity	W/m^2
T_0	Fluid's temperature in the absorbing unit (in the outlet section)	$^\circ$C
T_a	Ambient temperature	$^\circ$C
T_{amb}	Ambient air temperature	$^\circ$C
T_{cell}	Solar cell temperature	$^\circ$C
T_i	Fluid's temperature in the absorbing unit (in the inlet section)	$^\circ$C
T_p	Plate temperature	$^\circ$C
T_s	Surface temperature	$^\circ$C
U_T	The heat transfer coefficient from solar cell to ambient air by considering the cover of the glass	Unitless
U_{top}	Total heat transfer coefficient from the solar cell to the ambient atmosphere through the glass	Unitless
V_{mp}	Maximum voltage of panel	Volt
V_{oc}	Open-circuit voltage	Volt

Latin symbols with superscripts:

Mathematical notation	Definition	Unit
$\dot{m}$	Mass flow rate	kg/s

Latin symbols with both subscripts and superscripts:

Mathematical notation	Definition	Unit
$\dot{Ex}_{electrical}$	Electrical exergy	J
$\dot{Ex}_{in}$	Total input exergy rate	kW
$\dot{Ex}_{out}$	Net output exergy rate	kW
$\dot{Ex}_{thermal}$	Thermal exergy	J
$\dot{Q}_u$	Rate of useful heat absorbed by the panel	kJ/kW

Abbreviations

Abbreviation	Definition
ANFIS	Adaptive neuro-fuzzy inference system
BIPV/T	Building-integrated photovoltaic/thermal
FF	Fill factor
GA	Genetic algorithm
MEAs	Multiobjective evolutionary algorithms
MOEA/D	Multiobjective evolutionary algorithm based on decomposition
MOPs	Multiobjective optimization problems
MOPSO	Multiobjective particle swarm optimization
MPPT	Maximum power point tracking
NSGA	Non-dominated sorting genetic algorithm
PCM	Phase change material
PV/T	Photovoltaic/thermal

References

1. Dincer, I.; Al-Muslim, H. Thermodynamic analysis of reheat cycle steam power plants. *Int. J. Energy Res.* **2001**, *25*, 727–739. [CrossRef]
2. Jin, H.; Ishida, M.; Kobayashi, M.; Nunokawa, M. Exergy evaluation of two current advanced power plants: Supercritical steam turbine and combined cycle. *J. Energy Resour. Technol.* **1997**, *119*, 250–256. [CrossRef]
3. Vuong, E.; Kamel, R.S.; Fung, A.S. Modelling and simulation of BIPV/T in EnergyPlus and TRNSYS. *Energy Procedia* **2015**, *78*, 1883–1888. [CrossRef]
4. Xu, L.; Luo, K.; Ji, J.; Yu, B.; Li, Z.; Huang, S. Study of a hybrid BIPV/T solar wall system. *Energy* **2020**, *193*, 116578. [CrossRef]
5. Yang, T.; Athienitis, A.K. Experimental investigation of a two-inlet air-based building integrated photovoltaic/thermal (BIPV/T) system. *Appl. Energy* **2015**, *159*, 70–79. [CrossRef]
6. Chinipardaz, M.; Amraee, S. Study on IoT networks with the combined use of wireless power transmission and solar energy harvesting. *Sādhanā* **2022**, *47*, 1–16. [CrossRef]
7. Shahsavar, A.; Talebizadeh, P.; Tabaei, H. Optimization with genetic algorithm of a PV/T air collector with natural air flow and a case study. *J. Renew. Sustain. Energy* **2013**, *5*, 023118. [CrossRef]
8. Cao, Y.; Kamrani, E.; Mirzaei, S.; Khandakar, A.; Vaferi, B. Electrical efficiency of the photovoltaic/thermal collectors cooled by nanofluids: Machine learning simulation and optimization by evolutionary algorithm. *Energy Rep.* **2022**, *8*, 24–36. [CrossRef]
9. Karathanassis, I.K.; Papanicolaou, E.; Belessiotis, V.; Bergeles, G.C. Multi-objective design optimization of a micro heat sink for Concentrating Photovoltaic/Thermal (CPVT) systems using a genetic algorithm. *Appl. Therm. Eng.* **2013**, *59*, 733–744. [CrossRef]
10. Khaki, M.; Shahsavar, A.; Khanmohammadi, S.; Salmanzadeh, M. Energy and exergy analysis and multi-objective optimization of an air based building integrated photovoltaic/thermal (BIPV/T) system. *Sol. Energy* **2017**, *158*, 380–395. [CrossRef]
11. Vera, J.T.; Laukkanen, T.; Sirén, K. Multi-objective optimization of hybrid photovoltaic–thermal collectors integrated in a DHW heating system. *Energy Build.* **2014**, *74*, 78–90. [CrossRef]
12. Singh, S.; Agarwal, S.; Tiwari, G.N.; Chauhan, D. Application of genetic algorithm with multi-objective function to improve the efficiency of glazed photovoltaic thermal system for New Delhi (India) climatic condition. *Sol. Energy* **2015**, *117*, 153–166. [CrossRef]
13. Sohani, A.; Dehnavi, A.; Sayyaadi, H.; Hoseinzadeh, S.; Goodarzi, E.; Garcia, D.A.; Groppi, D. The real-time dynamic multi-objective optimization of a building integrated photovoltaic thermal (BIPV/T) system enhanced by phase change materials. *J. Energy Storage* **2022**, *46*, 103777. [CrossRef]
14. Sarhaddi, F.; Farahat, S.; Ajam, H.; Behzadmehr, A.; Adeli, M.M. An improved thermal and electrical model for a solar photovoltaic thermal (PV/T) air collector. *Appl. Energy* **2010**, *87*, 2328–2339. [CrossRef]
15. Sattar, M.; Rehman, A.; Ahmad, N.; Mohammad, A.; Al Ahmadi, A.A.; Ullah, N. Performance Analysis and Optimization of a Cooling System for Hybrid Solar Panels Based on Climatic Conditions of Islamabad, Pakistan. *Energies* **2022**, *15*, 6278. [CrossRef]
16. Dasheng, L. Multi Objective Particle Swarm Optimization: Algorithms and Applications. Ph.D. Thesis, National University of Singapore, Singapore, 2009.
17. Zhang, Q.; Li, H. MOEA/D: A multiobjective evolutionary algorithm based on decomposition. *IEEE Trans. Evol. Comput.* **2007**, *11*, 712–731. [CrossRef]
18. Mishra, R.; Tiwari, G. Energy and exergy analysis of hybrid photovoltaic thermal water collector for constant collection temperature mode. *Sol. Energy* **2013**, *90*, 58–67. [CrossRef]
19. Lee, J.H.; Hwang, S.G.; Lee, G.H. Efficiency improvement of a photovoltaic thermal (PVT) system using nanofluids. *Energies* **2019**, *12*, 3063. [CrossRef]
20. Aberoumand, S.; Ghamari, S.; Shabani, B. Energy and exergy analysis of a photovoltaic thermal (PV/T) system using nanofluids: An experimental study. *Sol. Energy* **2018**, *165*, 167–177. [CrossRef]
21. Weather Spark, The Weather Year Round Anywhere on Earth, Cedar Lake Ventures, Inc. Available online: www.weatherspark.com (accessed on 1 February 2021).